Fibers and Polymers 2016, Vol.17, No.2, 282-288
DOI 10.1007/s12221-016-5611-z

ISSN 1229-9197 (print version)
ISSN 1875-0052 (electronic version)

Investigations on Mechanical Characteristics of Glass Fiber Reinforced Epoxy Composite Modified with Amino-terminated Hyperbranched Polymer

Shuiping Li[1,2]*, Qing Lin[3], Huajun Zhu[1], Chong Cui[2]*, Haijun Hou[1], Tingting Lv[1], and Yanbo Li[1]

[1]*School of Materials Engineering, Yancheng Institute of Technology, Jiangsu 224051, P. R. China*
[2]*College of Materials Science and Engineering, Nanjing University of Science and Technology, Jiangsu 210094, P. R. China*
[3]*College of Materials Engineering, Jinling Institute of Technology, Jiangsu 211169, P. R. China*
(Received August 14, 2015; Revised December 30, 2015; Accepted January 30, 2016)

Abstract: Glass fiber, GF, which was first hydroxylated and silanized, was incorporated into epoxy resin modified with amino-terminated hyperbranched polymer (ATHBP) to obtain high performance composite. The effects of GFs content on the mechanical properties of composites were investigated, discussing the results from flexural, tensile, and impact tests. The composites revealed noticeable improvement in flexural strength, tensile strength as well as impact strength but slow decrease in elongation at break, compared to the epoxy/ATHBP thermoset. FESEM morphology results indicated the good compatibility between epoxy matrix and GF in the appearance of ATHBP and showed that the toughening mechanism was mainly attributed to the stress transfer mechanism.

Keywords: Composite, Fiber, Hyperbranched polymer, Mechanical property, Toughness

Introduction

It is well known that epoxies are widely used for structure applications, polymer matrixes, coatings, and adhesives due to the excellent mechanical performances, low shrinkage on curing, high chemical and corrosion resistances, and ease of processability under a variety of conditions [1-4]. However, the use of epoxy thermosets is often limited by their inherent brittleness and poor resistance to crack initiation and propagation [5-14]. Hence, it is necessary to improve the toughness of epoxy resins. Seas of modifier or fillers have been used to toughen the epoxy thermosets/composites, such as reactive rubber [15], thermoplastic polymer [16], copolymers [17,18], nanoparticles [19,20], and core-shell particles [21,22]. However, the improvement of toughness through the incorporation of these materials is achieved at the cost of mechanical properties, glass transition temperature (Tg) and processability [23].

Hyperbranched polymers (HBPs) as a subfamily of dendritic polymers, which also contain a high density and variety of functional terminal groups, are highly branched macromolecules with a unique 3-D architecture [24]. HBPs, which generally exhibit lower viscosity than linear polymers of the same molar mass [24], have been incorporated into epoxy resins to fabricate epoxy thermosets with high toughness [14,23,25-32]. The high density of functional terminal groups and a lot amount of free volumes and spaces in the architecture of HBPs are the major two excellent characteristics for HBPs to improve the toughness of epoxy resins [26]. However, the limits of improving epoxy resins properties through the addition of HBPs have been reached, since the thermosets properties achieved generally involve compromises [4]. For example, toughness is obtained at the cost of mechanical properties or glass transition temperature [26,33]. Hence, efforts have been directed at determining effective methods to improve the mechanical performances of these thermosets [34-40]. But, the improvement of mechanical properties of epoxy thermosets through inorganic particles has not translated directly into tougher thermosets. Therefore, research in this area is still in progress.

Researchers have attempted to improve the properties of epoxy resins via adding carbon fibers [4,41-45], carbon nanotubes [46-48] and graphemes [49,50]. But the expensive cost of carbon fibers, carbon nanotubes and grapheme restricts the widely and general utility applications. It is widely known that glass fiber (GF) is a kind of general and low-cost fibers and exhibits substantially mechanical properties when it is used as reinforcing filler, especially for epoxy resins [20]. In the present work, epoxy/HBP thermoset was prepared to use as matrix materials with GFs. GF was hydroxylated and silanized to enhance the compatibility between GF and matrix. The influences of GFs on the mechanical performances of epoxy composites were investigated, discussing the results from flexural, tensile and impact tests. FESEM technique was used to observe the impact fracture surfaces of composites for discussing the toughening mechanisms.

Experimental

Materials

An aqueous of H_2O_2 (30 wt %), succinic anhydride (98 %), diethanolamine (98 %), diethylenetriamine (98 %), toluene (98 %) and N,N-dimethylformamide (98 %) were purchased from Chengdu Kelong Chemical Reagent Company, China. γ-Aminopropyl triethoxysilane (γ-APS, 98 %) was obtained from Sinopharm Chemical Reagent Co., Ltd., China. All reagents were used as received. Diglycidyl ether of bisphenol-

*Corresponding author: lishuiping2002@126.com
*Corresponding author: cuichongnust@163.com

A epoxy resin E51 with an epoxide equivalent of 185-208 g/eq was purchased from Hangzhou Wuhuigang Adhesive Co., Ltd., China. Hardener, polyamide 650, which had an amine value of 220±20 mgKOH/g, was supplied by Wuxi Resin Factory, China. Glass-fibers, GFs, with a diameter of 10 μm and an average length of 30 μm were supplied by Corker CO., Ltd., Taikang, China.

Synthesis of Amino-terminated Hyperbranched Polymer (ATHBP)

Hyperbranched polymer with terminal hydroxyl group, which was synthesized through a polymerization of AB_2 approach with succinic anhydride and diethanolamine [26], was end-capped by diethylenetriamine to fabricate amino-terminated hyperbranched polymer (ATHBP). In a few words, 1.57 g of succinic anhydride and 1.50 g of diethanolamine were added into a 50 m*l* three-necked round-bottomed flask with a thermometer and heated to 70 ºC for 6 h under magnetic stirring. Then, the melting mixture was heated to 120 ºC and stirred under nitrogen for another 6 h. Then this system was vacuumed for 2 h to remove the moisture. After that, the initial products were heated to 110 ºC and 3.0 g of diethylenetriamine was added dropwise and then stirred for 10 h. This reaction was also protected by nitrogen atmosphere. The final products were redissolved in N,N-dimethylformamide and centrifuged at 5000 rpm for 5 min to remove the unreacted residues. After dried under vacuum at 80 ºC for 12 h, ATHBP was obtained.

Fabrication of Epoxy Composites with Silanized Glass Fibers

GFs were first dried at 105 ºC for 3 h in an oven to remove the moisture. Then 0.5 g of GFs were added into a 25 m*l* three-neck round-bottom flask with 5 m*l* of H_2O_2 and refluxed at 105 ºC for 4 h under magnetic stirring. The fibers were recovered by centrifugation at 5000 rpm for 10 min and washed with deionized water three times. After dried under vacuum at 80 ºC overnight, the fibers were added into 5 m*l* of toluene and sonicated for 30 min, and then 0.25 g of γ-Aminopropyl triethoxysilane was added and the mixture was heated to 80 ºC for 24 h under nitrogen flow and magnetic stirring. The products were recovered by centrifugation at 5000 rpm for 10 min and washed with toluene water three times and dried under vacuum at 80 ºC for 12 h. The products were named as silanized GFs.

Different amount of silanized GFs were blended with epoxy (GFs/E51, 0-5 wt %) by mechanical stirring for 20 min. Then, ATHBP (ATHBP/E51, 20 wt %) was added into the blends and stirred for 10 min. A certain amount of polyamide 650 (Polyamide/E51, 120/100 wt/wt), which was preheated to 60 ºC to improve the processability, was added into the mixtures and also stirred for 10 min, followed by pouring into a stainless steel template and cured at 60 ºC for 48 h in an oven.

Characterization

Attenuated total internal reflectance infrared (ATR-IR) spectroscopy spectra were conducted with a Tensor 37 instrument (Germany, Bruker) at a resolution of 4 cm^{-1} with 32 scans over the range of 4000-400 cm^{-1}. ^1H nuclear magnetic resonance (^1H NMR) spectroscopy spectrum were recorded on a AVANCE III 500 NMR spectrometer (Switzerland, Bruker) with deuterated dimethyl sulfoxide ($DMSO\text{-}d_6$) as the solvent at 293 K and tetramethylsilane (TMS) as an internal standard. Tensile tests were performed on dog-bone shaped type according to GB/T 2567-2008 with an SHIMADZU AG-X plus test machine. Un-notch impact tests were performed with a ZBC 50 pendulum impact testing machine (China, New SANS), according to GB/T 2567-2008 standard of a thickness of 4 mm and a width of 10 mm. All of the presented results were an average of five specimens. FESEM was recorded using a Hitachi SU8000 field-emission scanning electron microscope (Japan, Hitachi), and the fracture surfaces of the composites were sputter-coated with gold before observation.

Results and Discussion

Characterization of ATHBP

The ATR-IR spectrum of ATHBP is shown in Figure 1. The two weak peaks at 1027 and 1064 cm^{-1} are assigned to the stretching vibration of C-N. The band at 1295 cm^{-1} is attributed to the bending vibration of C-O. Otherwise, the band at 1462 cm^{-1} is related to the bending vibration of C-H. The strong peak appears at 1555 cm^{-1} that is characteristic of N-H bending vibration. The peak at 1638 cm^{-1} can be ascribed to amide C=O stretching [29]. Peaks appear at 2851 and 2944 cm^{-1} that are characteristic of symmetric and asymmetric C-H stretching vibration of $-CH_2$. The weak band at 3092 cm^{-1} is assigned to the asymmetric stretching of CH. And the peak at 3287 cm^{-1} is ascribed to the symmetric stretching of -NH. These appearances of bands at 1027,

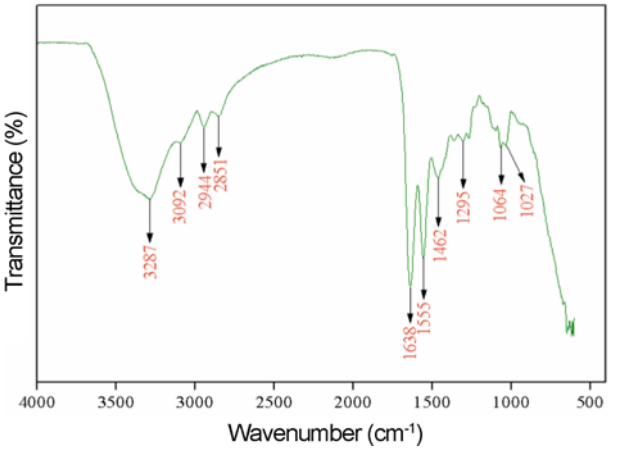

Figure 1. ATR-IR spectrum of ATHBP.

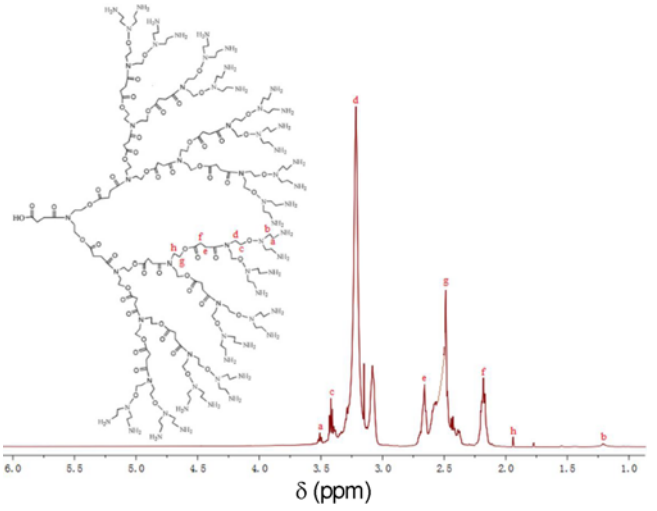

Figure 2. ^{1}H NMR spectrum of ATHBP.

1064, 1555 and 3287 cm^{-1} may indicate the successful synthesis of amino-terminated hyperbranched polymer.

The ^{1}H NMR spectrum of ATHBP provides more detailed and direct evidence to prove the successful synthesis of ATHBP (Figure 2). The characteristic peaks from the amide protons are clearly detected in the ^{1}H NMR spectrum of ATHBP. The spectrum presents characteristic chemical shifts of protons in the framework of ATHBP at 3.503 ppm (N-CH_2-C**H**$_2$-NH_2), 1.216 ppm (N-C**H**$_2$-CH_2-NH_2), 3.414 ppm (N-CH_2-C**H**$_2$-N), 3.222 ppm (N-C**H**$_2$-CH_2-N), 2.665 ppm (CH_2-C**H**$_2$-C), 2.188 ppm (C-C**H**$_2$-CH_2-), 2.533 ppm (N-CH_2-C**H**$_2$-O), and 1.879 ppm (N-C**H**$_2$-CH_2-O). And the ^{1}H NMR spectrum shows three kinds of proton peaks, which can be attributed to linear, dendritic and terminal units. For details, the peaks at 1.879, 2.188, 2.533 and 2.665 ppm are attributed to the amide protons of the linear units, the peaks at 3.222 and 3.414 ppm are assigned to the amide protons of the dendritic units and the peak at 1.216 and 3.503 ppm are ascribed to the amide protons of the terminal units. The results of ATR-IR and ^{1}H NMR may certainly suggest the successfully synthesis of amino-terminated hyperbranched polymer.

ATR-IR of Epoxy Thermoset/composite

The progress of reaction among epoxy unite, ATHBP and GF is studied by ATR-IR spectroscopy and the resulting spectra are shown in Figure 3. In the spectrum of epoxy/ATHBP thermoset, the appearance of the weak band at 1503 cm^{-1} is assigned to the C-H bending vibration. The peaks at 1185, 1101, and 1037 cm^{-1} are attributed to the stretching vibration of the ester group, -C-O stretching and C-O-C stretching vibrations [51], which indicate the existence of ester groups in the thermoset backbone. The appearance of the absorption band at 832 cm^{-1} confirms the presence of oxirane group. Compared to the spectrum of epoxy thermoset,

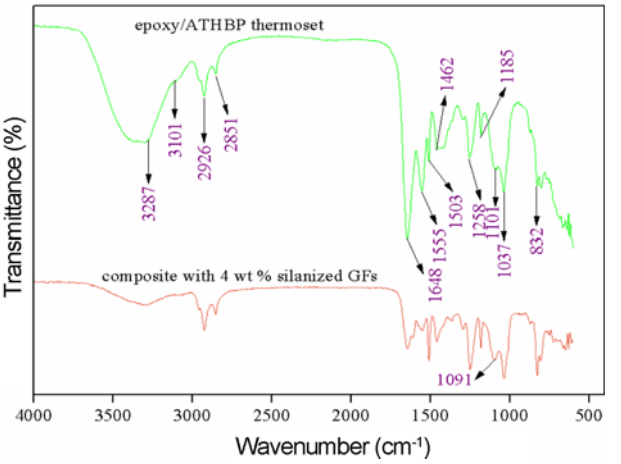

Figure 3. ATR-IR spectra of epoxy/ATHBP thermoset (a) and composite with 4 wt % GFs (b).

the significant difference in the spectrum of the composite with 4 wt % silanized GFs is the present of the absorption band at 1091 cm^{-1}, which is ascribed to asymmetrical stretching vibration of Si-O-Si. This result approves that the ATHBP and silanized GF have already been incorporated into the network of epoxy matrixes.

Mechanical Properties

It is well known that the improvement of toughness of epoxy resins by addition of HBPs is obtained at the cost of mechanical properties [26]. So some filler should be incorporated into epoxy/HBP themosets to fabricate composite with high mechanical performance and toughness. The flexural strength, tensile strength, percent elongation at break, and impact strength of composites as function of silanized GFs content are illustrated in Figure 4-7, respectively. It is accordance with the above description and our former report [26] that the flexural strength value decreases with the addition of

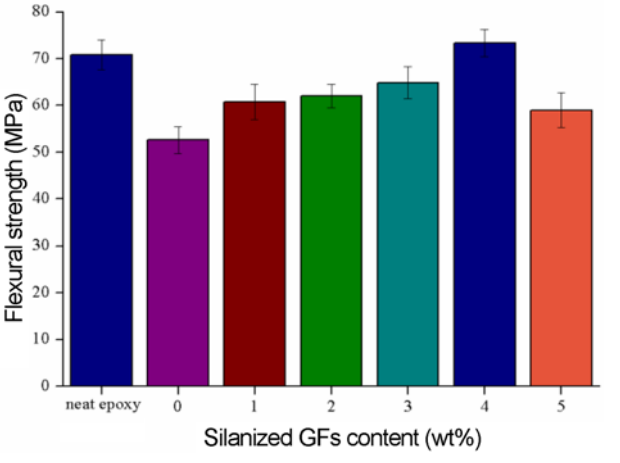

Figure 4. Flexural strengths of composites as function of GFs content.

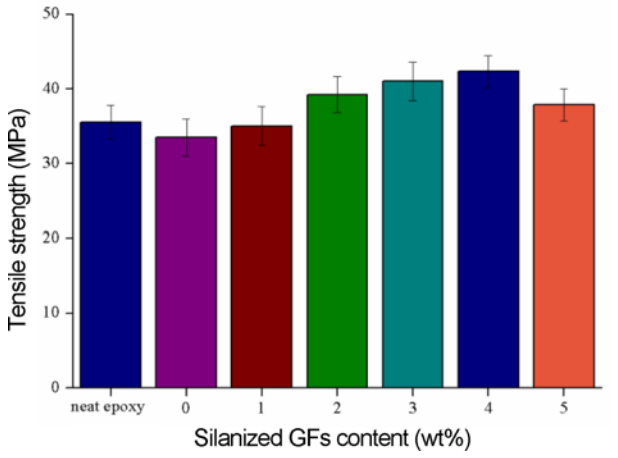

Figure 5. Tensile strengths of composites as function of GFs content.

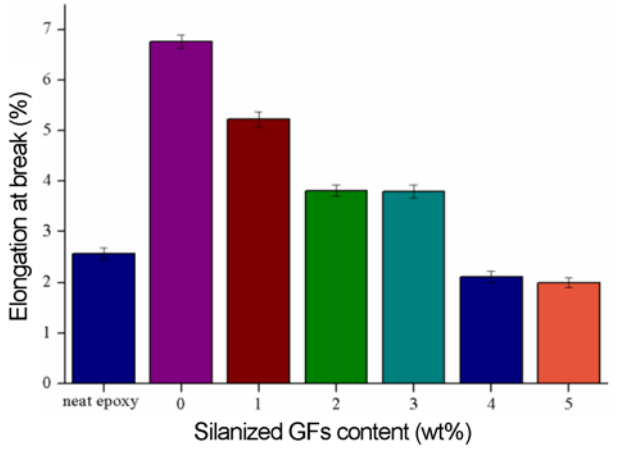

Figure 6. Elongation at break of composites as function of GFs content.

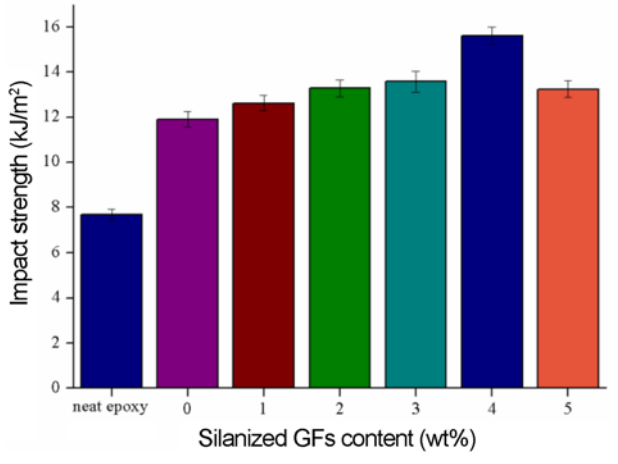

Figure 7. Impact strengths of composites as function of GFs content.

ATHBP (Figure 4), which may be due to the introduction of the flexible chain in ATHBP structure. In contrast, the flexural strength increases from 52.59 MPa for epoxy/ATHBP thermoset to 73.34 MPa for the composite with 4 wt % silanized GFs, which increases by about 39.5 %. Because epoxy matrixes transfer stress to fibers, GFs can generally carry the load imposed on the composites [52].

The introduction of ATHBP just slightly decreases the tensile strength of thermoset, as shown in Figure 5. However, tensile strength of composite increases with increment of GFs contents. The highest tensile strength of composites, formulation with 4 wt % GFs, increases by about 26.4 %, compared to the epoxy/ATHBP thermoset. The improvement of the tensile strength of composite may be attributed to the good adhesion of fiber-matrix interfaces [53], which have sufficient interfacial strength for loads transfer [52]. The introduction of flexible chains, which are contained in the structure of ATHBP and result in a decrease of flexural strength of epoxy/ATHBP thermoset, can sharply enhance the percent elongation at break (Figure 6). In contrast, the elongation decreases with increment of silanized GFs, which is due to the inhibition of GFs to the extension of flexible chains.

As shown in Figure 7, the introduction of ATHBP can exceptionally improve the impact strength of epoxy resins. For instance, the impact strength of epoxy/ATHBP thermoset increases by about 55.3 %, compared to the neat epoxy thermoset. Moreover, the impact strength also increases steadily by the addition of silanized GFs. The highest impact strength of composites, the formulation for 4 wt % silanized GFs, is higher than 104 and 31.2 %, compared to the neat epoxy and epoxy/ATHBP thermosets. It should be noticed that the impact strength decreases when the GFs content increases to 5 wt % but also higher than the neat epoxy and epoxy/ATHBP thermosets. These results indicate that the toughness of epoxy thermosets modified with ATHBP can be enhanced by the incorporation of GFs.

It can be concluded that 4 wt % is the optimum percentage for silanized GFs incorporated into epoxy/ATHBP thermosets, to obtain the maximum mechanical properties and excellent toughness. This improvement of mechanical performances and toughness of epoxy composites can be explained as follows: firstly, the incorporation of glass fibers makes crack and/or shearing deformation deflecting [52]; secondly, GFs, which are embedded into the epoxy matrixes, can carry load from the matrixes when the matrixes are under loading; thirdly, the reaction between epoxy units and amino-terminated groups attaching to the surface of ATHBP is contributed to improve the toughness of epoxy composites [14]. Fourthly, the introduction of ATHBP enhance the ductility of composite and hinder crack initiation and propagation; lastly, ATHBP enhances the compatibility between epoxy matrixes and silanized GFs, which is due to the high density of reactive terminal groups in the framework of

ATHBP, and thus improves the stress transfer to glass fibers and results to improve the reinforcement efficiency of GFs. The decreases of flexural strength, tensile strength and impact strength of the formulation with 5 wt % GFs are owing to the aggregation of GFs when the fiber concentration is above the percolation threshold value [54]. Aggregation can reduce the fiber-matrix interfacial strength and induce stress concentration to generate macrocracks then result in decreases of mechanical properties and toughness of epoxy composites [21,55].

Morphology of Epoxy Thermoset/composites

Epoxy-based composites performance is based on the epoxy matrix, filler, and filler-matrix interfacial strength [1]. Effective load transfer from the matrix to the reinforcing phase requires sufficient bonding at the interfaces [1,56]. Therefore, interface adhesion between the matrix and fiber is important for the composite performance. The morphologies of the impact fracture surfaces of the neat epoxy, epoxy/ATHBP thermoset, and composites with 4 wt % silanized GFs are investigated by FESEM analyses and shown in Figure 8. In Figure 8(a), we report the fracture surface FESEM image of the neat epoxy sample. The fracture surface is relatively smooth and glassy, only presents a few cracks in the same direction, showing the typical morphology of a brittle thermosetting polymer, which is poor resistance to crack initiation and propagation. In Figure 8(b) we show the fracture surface of FESEM image of the epoxy/ATHBP thermoset. In this case, it is possible to see a rougher surface, which contains high amount of cracks and shear yielding and result in absorbing more fracture energy and then improve the impact resistance of epoxy thermoset [30]. It shows that the toughness mechanism of ATHBP is attributed to the shearing deformation mechanism. In Figure 8(c) and 8(d), we show the impact fracture surface of FESEM images of epoxy composite with 4 wt % silanized glass fibers. The fracture surfaces present lots amount of micro-shearing deformations, which is due to the stress transfer and concentration onto and/or around the glass fibers. Furthermore, it can be clearly observed that the silanized GFs are embedded vertically (Figure 8(c)) and horizontally (Figure 8(d)) in epoxy matrixes. Moreover, the marked region, which is magnified and inserted in Figure 8(c), indicates the notable compatibility between epoxy matrixes and silanized GFs in the present of ATHBP. In addition, the stress concentration around glass fiber may result to crack initiation and propagation [57], which is marked lightly in Figure 8(d) and the inserted graph of silanized GFs is used to conform the appearance of GFs. It can conclude that the toughness mechanism of GFs is based on the stress transfer mechanism.

Conclusion

It was well known that the addition of hyperbranched polymers could exceptionally improve the toughness of epoxy resins but sacrificed other mechanical properties. In this paper, silanized glass fibers were incorporated into epoxy/ATHBP thermosets to fabricate high performance composites. The mechanical properties of the prepared composites were compared with the neat epoxy and epoxy/

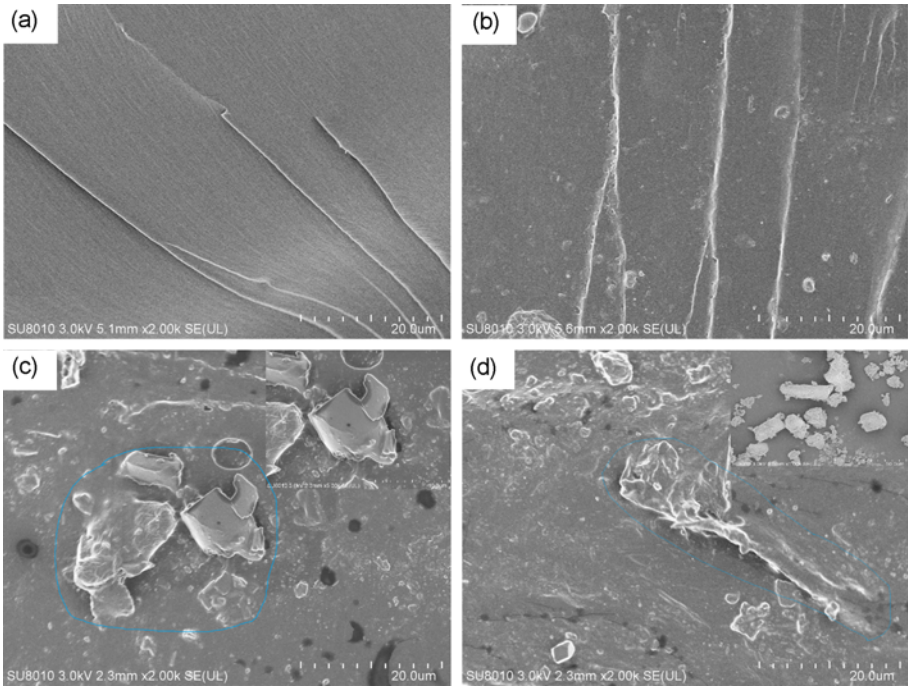

Figure 8. FESEM images of the neat epoxy (a), epoxy/ATHBP thermoset (b), and composite with 4 wt % GFs (c-d).

ATHBP thermosets.

The results indicated that the addition of glass fibers could notably improve the flexural strength, tensile strength as well as impact resistance of epoxy thermosets modified with amino-terminated hyperbranched polymers. FESEM analysis showed the good compatibility between epoxy matrixes and glass fibers in the present of ATHBP. The toughness mechanisms of ATHBP and GF are shearing deformation mechanism and stress transfer mechanism, respectively.

Acknowledgements

The authors gratefully acknowledge supports from the National Science and Technology Major Project of the Ministry of Science and Technology of China (2012ZX04010032), the National Natural Science Foundation of China (51402251, 51578289 and 51502259), the joint research fund between Collaborative Innovation Center for Ecological Building Materials and Environmental Protection Equipments and Key Laboratory for Advanced Technology in Environmental Protection of Jiangsu Province (GX2015107), a project funded by the Flagship Major Development of Jiangsu Higher Education Institutions (PPZY2015A025)and the Natural science fund of Jiangsu Province (BK20130428).

References

1. P. Punchaipetch, N. A. D'Souza, W. Brostow, and J. T. Smith, *Polym. Compos.*, **23**, 564 (2002).
2. Y. X. Zhou, M. A. Baseer, H. Mahfuz, and S. Jeelani, *Mater. Sci. Eng. A-Struct. Mater. Prop.*, **420**, 63 (2006).
3. E. Bozkurt, E. Kaya, and M. Tanoglu, *Compos. Sci. Technol.*, **67**, 3394 (2007).
4. Y. Xu and S. Van Hoa, *Compos. Sci. Technol.*, **68**, 854 (2008).
5. S.-R. Ha, K.-Y. Rhee, S.-J. Park, and J. H. Lee, *Compos. Pt. B-Eng.*, **41**, 602 (2010).
6. H.-Y. Liu, G.-T. Wang, Y.-W. Mai, and Y. Zeng, *Compos. Pt. B-Eng.*, **42**, 2170 (2011).
7. H. J. Kim, D. H. Jung, I. H. Jung, J. I. Cifuentes, K. Y. Rhee, and D. Hui, *Compos. Pt. B-Eng.*, **43**, 1743 (2012).
8. A. Fereidoon, M. Rajabpour, and H. Hemmatian, *Compos. Pt. B-Eng.*, **54**, 400 (2013).
9. J. Liu, H.-J. Sue, Z. J. Thompson, F. S. Bates, M. Dettloff, G. Jacob, N. Verghese, and H. Pham, *Acta Mater.*, **57**, 2691 (2009).
10. Y. Fu, H. Liu, and W. H. Zhong, *Colloid Surf. A-Physicochem. Eng. Asp.*, **369**, 196 (2010).
11. X. Gu, X. Huang, H. Wei, and X. Tang, *Eur. Polym. J.*, **47**, 903 (2011).
12. M. Bashar, U. Sundararaj, and P. Mertiny, *Compos. Pt. A-Appl. Sci. Manuf.*, **43**, 945 (2012).
13. M. T. Bashar, U. Sundararaj, and P. Mertiny, *Polym. Eng. Sci.*, **54**, 1047 (2014).
14. L. Pan, S. Lu, X. Xiao, Z. He, C. Zeng, J. Gao, and J. Yu, *Rsc Adv.*, **5**, 3177 (2015).
15. W. Zhou and J. Cai, *J. Appl. Polym. Sci.*, **124**, 4346 (2012).
16. S. Grishchuk, O. Gryshchuk, M. Weber, and J. Karger-Kocsis, *J. Appl. Polym. Sci.*, **123**, 1193 (2012).
17. X. Q. Xu, L. Zhou, B. Liang, Y. M. Wu, and C. S. Wang, *Polym.-Plast Technol. Eng.*, **53**, 753 (2014).
18. C. Hu, J. Yu, J. Huo, Y. Chen, and H. Ma, *Compos. Pt. A-Appl. Sci. Manuf.*, **78**, 113 (2015).
19. D. Quan and A. Ivankovic, *Polymer*, **66**, 16 (2015).
20. D. Kim, I. Chung, and G. Kim, *Fiber. Polym.*, **14**, 2141 (2013).
21. X. L. Zeng, S. H. Yu, R. Sun, and J. B. Xu, *Compos. Pt. A-Appl. Sci. Manuf.*, **73**, 260 (2015).
22. W. Thitsartarn, X. Fan, Y. Sun, J. C. C. Yeo, D. Yuan, and C. He, *Compos. Sci. Technol.*, **118**, 63 (2015).
23. T. Liu, Y. Nie, L. Zhang, R. Chen, Y. Meng, and X. Li, *Rsc Adv.*, **5**, 3408 (2015).
24. C. Gao and D. Yan, *Prog. Polym. Sci.*, **29**, 183 (2004).
25. T. Liu, Y. Nie, R. Chen, L. Zhang, Y. Meng, and X. Li, *J. Mater. Chem. A*, **3**, 1188 (2015).
26. S. Li, C. Cui, H. Hou, Q. Wu, and S. Zhang, *Compos. Pt. B-Eng.*, **79**, 342 (2015).
27. S. Li, C. Cui, and H. Hou, *Colloid Polym. Sci.*, **293**, 2681 (2015).
28. C. Acebo, X. Fernandez-Francos, M. Messori, X. Ramis, and A. Serra, *Polymer*, **55**, 5028 (2014).
29. R. Qian, J. Yu, L. Xie, Y. Li, and P. Jiang, *Polym. Adv. Technol.*, **24**, 348 (2013).
30. G. G. Buonocore, L. Schiavo, I. Attianese, and A. Borriello, *Compos. Pt. B-Eng.*, **53**, 187 (2013).
31. T. Li, H. Qin, Y. Liu, X. Zhong, Y. Yu, and A. Serra, *Polymer*, **53**, 5864 (2012).
32. S. Li, H. Zhu, T. Lv, Q. Lin, H. Hou, Y. Li, Q. Wu, and C. Cui, *Colloid Polym. Sci.*, 10.1007/s00396-015-3811-5, (2015).
33. D. Foix, A. Serra, L. Amparore, and M. Sangermano, *Polymer*, **53**, 3084 (2012).
34. Y. Zhao, H. Zou, W. Shi, and L. Tang, *Microporous Mesoporous Mat.*, **92**, 251 (2006).
35. P. K. Maji, P. K. Guchhait, and A. K. Bhowmick, *ACS Appl. Mater. Interfaces*, **1**, 289 (2009).
36. L. Fogelström, E. Malmström, M. Johansson, and A. Hult, *ACS Appl. Mater. Interfaces*, **2**, 1679 (2010).
37. G. Das, R. D. Kalita, H. Deka, A. K. Buragohain, and N. Karak, *Prog. Org. Coat.*, **76**, 1103 (2013).
38. M. M. Eissa, M. S. A. Youssef, A. M. Ramadan, and A. Amin, *Polym. Eng. Sci.*, **53**, 1011 (2013).
39. B. Roy, P. Bharali, B. K. Konwar, and N. Karak, *Bioresource Technol.*, **127**, 175 (2013).
40. S. Pramanik, P. Bharali, B. K. Konwar, and N. Karak, *Mater. Sci. Eng. C*, **35**, 61 (2014).
41. J.-S. Park, S.-S. Park, and S. Lee, *Macromol. Symposia*, **249-250**, 568 (2007).
42. F. An, C. X. Lu, Y. H. Li, J. H. Guo, X. X. Lu, H. B. Lu, S.

Q. He, and Y. Yang, *Mater. Des.*, **33**, 197 (2012).
43. N. T. Phong, M. H. Gabr, K. Okubo, B. Chuong, and T. Fujii, *Compos. Struct.*, **99**, 380 (2013).
44. G. C. Qi, S. Y. Du, B. M. Zhang, Z. W. Tang, and Y. L. Yu, *Compos. Sci. Technol.*, **105**, 1 (2014).
45. E. Farmand-Ashtiani, J. Cugnoni, and J. Botsis, *Int. J. Solids Struct.*, **55**, 58 (2015).
46. M. R. Irshidat, M. H. Al-Saleh, and H. Almashagbeh, *Mater. Des.*, **89**, 225 (2016).
47. S. P. Sharma and S. C. Lakkad, *Compos. Pt. A-Appl. Sci. Manuf.*, **69**, 124 (2015).
48. Y. Li and X. Huang, *Compos. Pt. A-Appl. Sci. Manuf.*, **78**, 166 (2015).
49. C. Y. Lee, J.-H. Bae, T.-Y. Kim, S.-H. Chang, and S. Y. Kim, *Compos. Pt. A-Appl. Sci. Manuf.*, **75**, 11 (2015).
50. C. M. Hadden, D. R. Klimek-McDonald, E. J. Pineda, J. A. King, A. M. Reichanadter, I. Miskioglu, S. Gowtham, and G. M. Odegard, *Carbon*, **95**, 100 (2015).
51. S. Allauddin, M. K. Akhil Chandran, K. K. Jena, R. Narayan, and K. V. S. N. Raju, *Prog. Org. Coat.*, **76**, 1402 (2013).
52. G. J. Withers, Y. Yu, V. N. Khabashesku, L. Cercone, V. G. Hadjiev, J. M. Souza, and D. C. Davis, *Compos. Pt. B-Eng.*, **72**, 175 (2015).
53. M. J. S. Zuberi and V. Esat, *Compos. Pt. B-Eng.*, **71**, 1 (2015).
54. R. P. Wang, T. Schuman, R. R. Vuppalapati, and K. Chandrashekhara, *Green Chem.*, **16**, 1871 (2014).
55. B. Qi, Q. X. Zhang, M. Bannister, and Y. W. Mai, *Compos. Struct.*, **75**, 514 (2006).
56. K. Fujiki, M. Sakamoto, S. Yoshikawa, T. Sato, and N. Tsubokawa, *Compos. Interface*, **6**, 215 (1998).
57. H. P. Konka, M. A. Wahab, and K. Lian, *Smart Mater. Struct.*, **21**, 1 (2012).